Available online at www.sciencedirect.com
SCIENCE DIRECT®
Journal of Solid State Chemistry 177 (2004) 366–371
JOURNAL OF SOLID STATE CHEMISTRY
http://elsevier.com/locate/jssc

Structure and thermal decomposition of sulfated β-cyclodextrin intercalated in a layered double hydroxide

Ji Wang, Min Wei, Guoying Rao, David G. Evans, and Xue Duan*

Key Laboratory of Science and Technology of Controllable Chemical Reactions, Ministry of Education, Beijing University of Chemical Technology, Applied Chemistry, Box 98, Beijing 100029, China

Received 30 April 2003; received in revised form 29 August 2003; accepted 7 September 2003

Abstract

The sodium salt of hexasulfated β-cyclodextrin has been synthesized and intercalated into a magnesium–aluminum layered double hydroxide by ion exchange. The structure, composition and thermal decomposition behavior of the intercalated material have been studied by variable temperature X-ray diffraction (XRD), Fourier transform infrared spectroscopy (FT-IR), inductively coupled plasma emission spectroscopy (ICP), and thermal analysis (TG-DTA) and a model for the structure has been proposed. The thermal stability of the intercalated sulfated β-cyclodextrin is significantly enhanced compared with the pure form before intercalation.

Keywords: Sulfated β-cyclodextrin; Layered double hydroxide; Intercalation; Structure; Thermal decomposition

1. Introduction

Layered double hydroxides (LDHs) are a class of anionic clays which can be represented by the general formula $[M^{II}_{1-x}M^{III}_{x}(OH)_2]^{x+}(A^{n-})_{x/n}\cdot mH_2O$ [1], where M^{II} and M^{III} are di- and tri-valent metal cations, respectively. LDHs have positively charged layers and a wide variety of charge-balancing anionic species, A^{n-}, have been intercalated into the gallery region. As a result, LDHs are now well established as excellent anion-exchange materials and their extensive intercalation chemistry has widespread applications in areas such as heterogeneous catalysis [2,3], optical materials [4,5], biomimetic catalysis [6,7], and separation science [8,9].

Cyclodextrins are cyclic oligosaccharides of *D*-glucopyranose that possess a unique structure containing a non-polar doughnut-shaped ring which can accommodate different kinds of compounds in the cavity [10–13]. Cyclodextrins and their derivatives are excellent "host" components for the microencapsulation of a wide variety of organic, as well as inorganic, guest molecules forming host–guest inclusion complexes in aqueous solution [10]. These compounds have prospective applications in a variety of fields including pharmaceuticals, cosmetics, the tobacco industry and environmental protection [10,14]. They also provide an excellent model system for mimicking the substrate–specific interaction of enzymes, and some of them are successful enzyme models [15,16]. The first report of the use of cyclodextrin as a "guest" component in layered solids was the incorporation of appropriately modified cyclodextrin in both Cu(II) montmorillonite and α-zirconium phosphate [17,18]. In 1998, Zhao and Vance reported the intercalation of carboxymethyl-β-cyclodextrin in LDHs as well as its sorption affinity for organic compounds [19,20].

Sulfated cyclodextrins have been widely used for enantiomeric separation, either by liquid chromatography using columns containing the materials bound to a solid support [21,22] or by capillary electrophoresis [23,24]. The intercalation of sulfated cyclodextrins in the confined interlayer region of LDHs should give rise to a new type of stationary phase for liquid chromatography with high chiral selectivity and low degree of leaching. Pinnavaia [25] has shown that sulfate ions intercalated in LDHs can be grafted to the layers by mild heating and if this is possible with the sulfated cyclodextrins their degree of leaching from the interlayer region could be further reduced. In this work, the hexasulfated β-cyclodextrin [represented as $NaSO_3$-β-CD(6)] has been intercalated into a magnesium–aluminum LDH.

*Corresponding author. Fax: +861064425385.
E-mail address: duanx@mail.buct.edu.cn (X. Duan).

0022-4596/$ - see front matter © 2003 Elsevier Inc. All rights reserved.
doi:10.1016/j.jssc.2003.09.006

The main purpose of this study was to investigate the interaction between the host layers and the guest as well as the thermal decomposition of the cyclodextrin after intercalation.

2. Experimental

2.1. Reagents

All chemicals including $Mg(NO_3)_2 \cdot 6H_2O$, $Al(NO_3)_3 \cdot 9H_2O$, NaOH, $NaNO_3$, Na_2CO_3, $CaCO_3$, ethanol, ether, acetone, sulfuric acid and β-cyclodextrin were analytical grade. β-cyclodextrin was purchased from Aldrich, and the others from the Beijing Chemical Plant Limited.

2.2. Synthesis of hexasulfated β-cyclodextrin, $NaSO_3$-β-CD(6)

$NaSO_3$-β-CD(6), $(C_{42}H_{64}O_{35})(SO_3Na)_6$, was synthesized according to the procedure described in the literature [26] and characterized by elemental analysis. Found (calculated): C 28.8 (28.9); H 4.2 (3.7); S 11.5 (10.9)%; C/S 6.7 (7.0).

2.3. Synthesis of SO_3-β-CD(6)/LDH

The precursor $[Mg_4Al_2(OH)_{12}](NO_3)_2 \cdot 4H_2O$, (Mg/Al-$NO_3$LDH) was synthesized by a procedure similar to that described previously [1]. A solution of $Mg(NO_3)_2 \cdot 6H_2O$ (32.0 g, 0.125 mol) and $Al(NO_3)_3 \cdot 9H_2O$ (11.7 g, 0.062 mol) in distilled, deionized water (200 cm^3) was added dropwise over 2 h to a solution of NaOH (12.5 g, 0.310 mol) and $NaNO_3$ (18.2 g, 0.210 mol) in water (250 cm^3). The mixture was held at 100°C for 36 h. The precipitate was separated by centrifugation, washed with water and dried at 60°C for 8 h. Found (calculated): Mg 17.2 (17.4); Al 9.5 (9.8); Mg/Al 2.1 (2.0).

The SO_3-β-CD(6)/LDH was obtained by the method of ion exchange. A solution of $NaSO_3$-β-CD(6) (1.5 g, 1 mmol) in distilled, deionized water (50 cm^3) was added to a suspension of Mg/Al-NO_3LDH (1.0 g, ca. 2 mmol) in distilled, deionized water (50 cm^3) and the mixture heated at 65°C under a nitrogen atmosphere for 39 h. The product was washed extensively with water, centrifuged and dried at 60°C. Found (calculated for $Mg_{0.70}Al_{0.30}(OH)_2(SO_3\text{-}\beta\text{-}CD(6))_{0.05}(CO_3)_{0.01}(NO_3)_{0.01} \cdot 0.04H_2O$): Mg 13.58 (13.68); Al 6.82 (6.75); C 20.33 (20.28); H 3.98 (4.64); S 7.69 (7.64); N 0.13 (0.14); Mg/Al 2.21 (2.25); C/S 7.06 (7.09).

2.4. Characterization

Powder X-ray diffraction (XRD) measurements were performed on a Rigaku XRD-6000 diffractometer, using Cu$K\alpha$ radiation ($\lambda = 0.154$ nm) at 40 kV, 30 mA. The samples as unoriented powders were scanned in steps of 0.02° in the 2θ range 3–70° using a count time of 4 s per step. The variable temperature XRD patterns of SO_3-β-CD(6)/LDH were obtained after heating the sample in the diffractometer for 20 min at the appropriate temperature.

Fourier transform infrared (FT-IR) spectra were recorded using a Bruker Vector22 spectrophotometer in the range 4000–400 cm^{-1} with 2 cm^{-1} resolution. The standard KBr disk method (1 mg of sample in 100 mg of KBr) was used.

Thermogravimetric analysis and differential thermal analysis (TG-DTA) were measured on a PCT-1A thermal analysis system with a heating rate of 10°C/min.

Metal analysis was performed with a Shimadzu ICPS-7500 instrument. C, H, N content was determined using an Elementarvario elemental analysis instrument.

3. Results and discussion

3.1. Determination of the degree of substitution of $NaSO_3$-β-CD

The sulfated cyclodextrin $NaSO_3$-β-CD was prepared by the literature method [26]. The degree of sulfation was determined from the carbon/sulfur ratio [22].

3.2. Structure of SO_3-β-CD(6)/LDH

The X-ray diffraction patterns of the original Mg/Al-NO_3LDH and the product of intercalation with $NaSO_3$-β-CD(6) are shown in Fig. 1. In each case, the reflections can be indexed to a hexagonal lattice with *R*-3*m* rhombohedral symmetry, commonly used for the description of LDH structures. Table 1 lists the basal spacings and lattice parameters. The value of the lattice

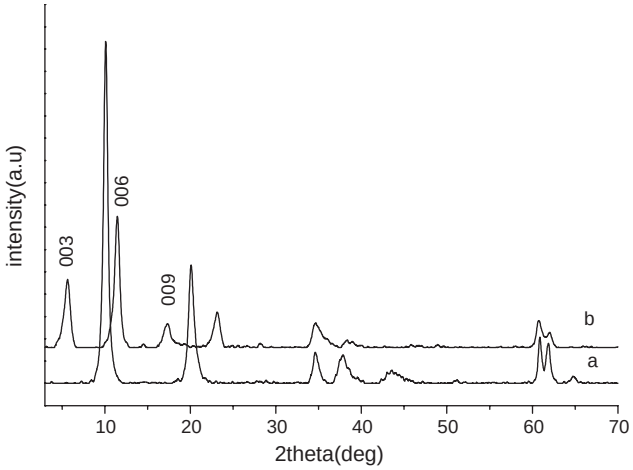

Fig. 1. XRD patterns of (a) Mg/Al-NO_3LDH and (b) SO_3-β-CD(6)/LDH.

Table 1
Lattice parameters for SO_3-β-CD(6)/LDH and Mg/Al-NO_3 LDH

Lattice parameter	SO_3-β-CD(6)/LDH	Mg/Al-NO_3LDH
d_{003}/nm	1.578	0.862
d_{006}/nm	0.773	0.440
d_{009}/nm	0.514	0.260
d_{110}/nm	0.152	0.152
Lattice parameter a/nm	0.305	0.305
Lattice parameter c/nm	4.733	2.286

parameter a is a function of the average distance between the metal ions and thus, since Al^{3+} is smaller than Mg^{2+}, gives an indication of the Mg^{2+}/Al^{3+} ratio. The value a of the intercalation product is identical to that of the precursor, 0.305 nm, indicating that there is no significant change in Mg^{2+}/Al^{3+} ratio on intercalation of SO_3-β-CD(6) anions. This is confirmed by analytical data (vide infra). The Mg/Al-NO_3LDH precursor has an XRD pattern similar to those reported previously [27,28], with an interlayer spacing (d_{003}) of 0.862 nm. After intercalation of SO_3-β-CD(6) anions, the interlayer distance increased to 1.578 nm. Since the thickness of the LDH hydroxide basal layer is 0.480 nm [28], the gallery height is 1.098 nm.

As shown in Fig. 1b, the strongest peak is the (006) reflection, while the (003) reflection has the strongest peak intensity in the diffraction pattern of the LDH precursor. This is possibly related to the presence of an LDH-CO_3^{2-} impurity phase which is often observed even when intercalation reactions are carried out under nitrogen. The peak around $2\theta = 11°$ may be a superposition of the (003) reflection of CO_3^{2-} LDH and the (006) reflection of SO_3-β-CD(6)/LDH, accounting for its enhanced intensity. The peak around $2\theta = 23°$can be assigned to the (006) reflection of CO_3^{2-}-LDH. This will be discussed further below. There are also very weak reflections around $2\theta = 14°$ and 28°, the origin of which is discussed below.

Cyclodextrin should be regarded as truncated cone rather than a cylinder [29]. There are seven primary and 14 secondary hydroxyl groups along the β-cyclodextrin cavity. The primary hydroxyl groups, which are located on the narrow side of the cyclodextrin ring, are more readily substituted than the secondary hydroxyl groups and therefore, for Na SO_3-β-CD(6), the six sulfate groups can be assumed to be on this side. β-cyclodextrin has an approximate torus thickness of 0.78 nm, an outer diameter of 1.53 nm and an inner diameter of 0.78 nm [29]. Considering the dimensions of the β-cyclodextrin molecule and the rule of charge balance, the SO_3-β-CD(6) anions can only adopt a monolayer arrangement with its cavity axis perpendicular to the LDH layer and sulfate groups on adjacent cyclodextrin molecules attached alternately to the upper and lower LDH layer surfaces. This is similar to the arrangement reported by Zhao and Vance for a tetradecasubstituted carboxymethyl-β-CD, where the gallery height was found to be 1.07 nm [19]. A schematic representation of the probable arrangement for SO_3-β-CD(6)/LDH is shown in Fig. 2.

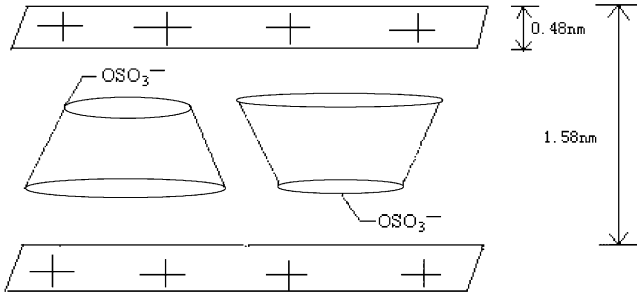

Fig. 2. A schematic representation of the possible arrangement for SO_3-β-CD(6)/LDH.

3.3. Chemical composition

Elemental analysis data suggest that the chemical composition of SO_3-β-CD(6)/LDH is $Mg_{0.70}Al_{0.30}(OH)_2(SO_3\text{-}\beta\text{-CD(6)})_{0.05}(CO_3)_{0.01}(NO_3)_{0.01} \cdot 0.04H_2O$. It can be seen that not all of the NO_3^- anions have been exchanged by SO_3-β-CD(6), which has been observed by other authors in studies of intercalation of large anions in Mg/Al-NO_3LDH precursors [30,31]. Some CO_3^{2-} containing LDH coexists with the SO_3-β-CD(6)/LDH, which is consistent with the XRD results. The total exclusion of carbonate from the interlayer space of LDHs is known to be difficult, which can be readily explained on the basis of the favorable lattice stabilization enthalpy associated with the small and highly charged CO_3^{2-} anions [32].

3.4. Investigation of the host–guest interaction by FT-IR spectroscopy

The FT-IR spectra of β-CD, $NaSO_3$-β-CD(6), Mg/Al-NO_3LDH and SO_3-β-CD(6)/LDH are shown in Fig. 3, and the main absorption bands are listed in Table 2.

Compared with β-CD [33] (Fig. 3a), the spectrum of $NaSO_3$-β-CD(6) (Fig. 3b) shows a strong band at 1267 cm^{-1} and a weak one at 1058 cm^{-1}, which can be attributed to SO_2 and C–O–S stretching vibrations, respectively [34]. A broad strong absorption band centered at 3427 cm^{-1} is observed, which can be attributed to the stretching vibrations of hydroxyl groups and physically adsorbed water [35]. The absorption at 2923 cm^{-1} is due to the stretching vibration of CH_2, and that at 1659 cm^{-1} results from the HOH bending of physically adsorbed water. Bands at 1159, 1027 and 943 cm^{-1} can be assigned to the vibration of C–O and C–O–C in the glucose units and the C–O–C ring vibrations, respectively [34].

The FT-IR spectrum of the Mg/Al-NO_3LDH (Fig. 3d) is similar to that reported in the literature

[27,28]. The very broad absorption band centered at 3467 cm^{-1} can be assigned to OH stretching vibrations of hydroxyl groups, water molecules in the interlayer, and physically adsorbed water [22]. The shoulder present at 2967 cm^{-1} is caused by hydrogen bonding of water to NO_3^- groups in the interlayer space, and the 1650 cm^{-1} band is mainly due to HOH bending of physically adsorbed water molecules [35]. By comparison with the spectrum of the LDH-nitrate precursor (Fig. 3d), the very broad absorption band centered at 3467 cm^{-1} in the spectrum of SO_3-β-CD(6)/LDH (Fig. 3c) can be assigned to OH stretching vibrations of hydroxyl groups, water molecules in the interlayer, and physically adsorbed water [35]. The absorption maxima at 1254 and 1059 cm^{-1} can be attributed to the stretching vibrations of SO_2 and C–O, respectively. Compared with $NaSO_3$-β-CD(6), the stretching vibrations of SO_2 and C–O in SO_3-β-CD(6)/LDH are shifted 13 and 5 cm^{-1} to low frequency, respectively. This may be related to the formation of hydrogen bonds between the SO_3-β-CD(6) anions and host layers and/or interlayer water molecules. The Al–O and Mg–O lattice vibrations can be observed at 826 and 668 cm^{-1} [36]. The absorption band at 1383 cm^{-1} can be assigned to a superposition of the NO_3^- and CO_3^{2-} stretching vibrations, in agreement with the XRD and elemental analysis data.

3.5. Thermal decomposition studied by variable temperature XRD and TG-DTA

The XRD patterns of SO_3-β-CD(6)/LDH calcined at various temperatures are shown in Fig. 4. The variation in the d_{003} basal spacing of SO_3-β-CD(6)/LDH with temperature is shown in Fig. 5. It can be observed in Fig. 4 that the 003, 006 and 009 diffraction peaks of SO_3-β-CD(6)/LDH move to higher angle with increasing temperature. There are two sharp decreases in the basal spacing as shown in Fig. 5. The first is from 20°C to 150°C with the value decreasing from 1.578 to 1.401 nm. This decrease is related to the destruction of

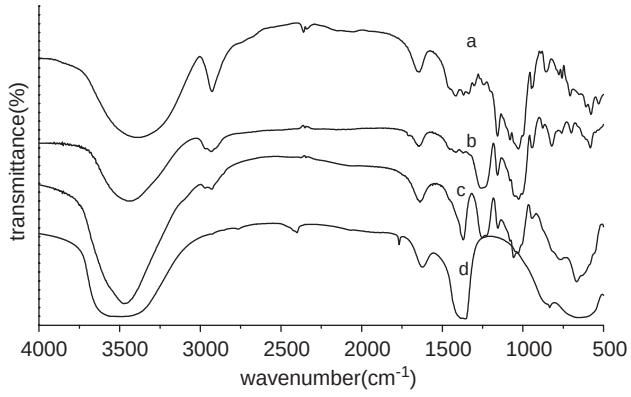

Fig. 3. IR spectra of (a) β-CD, (b) $NaSO_3$-β-CD(6), (c) SO_3-β-CD(6)/LDH and (d) Mg/Al-NO_3LDH.

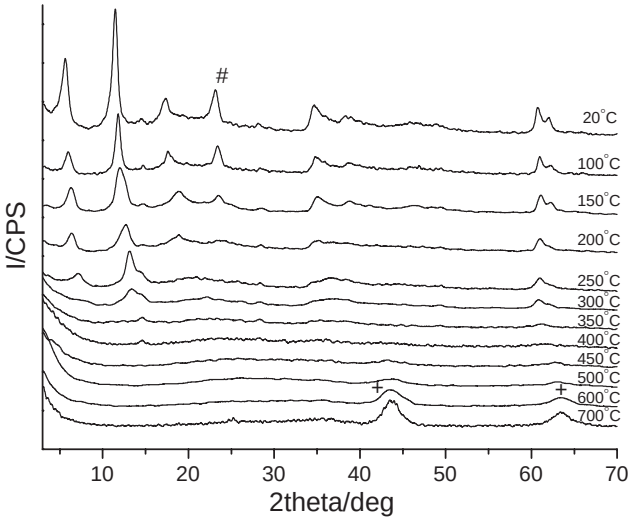

Fig. 4. XRD patterns of SO_3-β-CD(6)/LDH calcined at various temperatures.

Table 2
IR data for β-CD, $NaSO_3$-β-CD(6), SO_3-β-CD(6)/LDH and Mg/Al-NO_3LDH

Type of vibration/cm^{-1}	β-CD	$NaSO_3$-β-CD(6)	SO_3-β-CD(6)/LDH	Mg/Al-NO_3LDH
υ_{OH}	3343 (s)	3427 (vs)	3467 (vs)	3464 (s)
υ_{CH_2}	2923 (vs)	2923 (s)	2935 (w)	
δ_{CH_2}	1410 (m)	1410 (vw)		
δ_{OH}	1340 (m)	1340 (vw)		
υ_{C-O}	1156 (m)	1159 (m)	1155 (m)	
υ_{C-C} (skeletal stretching)	1079 (w)	1079 (w)	1079 (vw)	
υ_{C-O-C}	1027 (s)	1027 (m)	1027 (m)	
	946 (w)	943 (w)	942 (w)	
υ_{SO_2}		1267 (s)	1254 (s)	
υ_{S-O-C}		1058 (w)	1059 (s)	
			1383 (m)	1384 (vs)
Al-O (lattice vibration)			826 (w)	826 (w)
Mg-O (lattice vibration)			668 (s)	662 (s)

vs: very strong; s: strong; m: medium.; w: weak; vw: very weak.

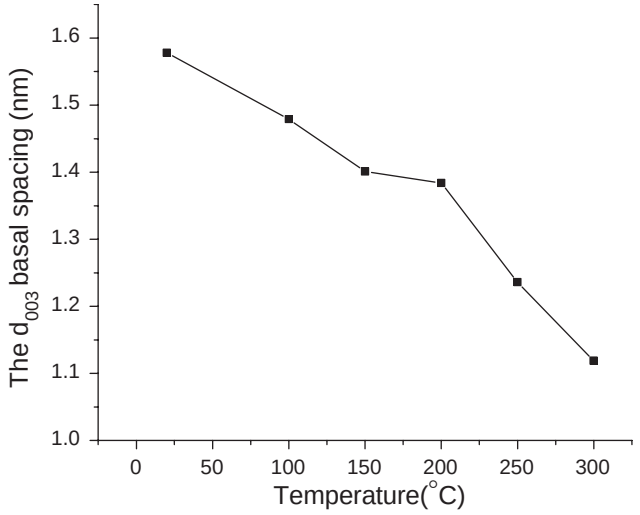

Fig. 5. The relationship between the d_{003} basal spacing and temperature for SO_3-β-CD(6)/LDH.

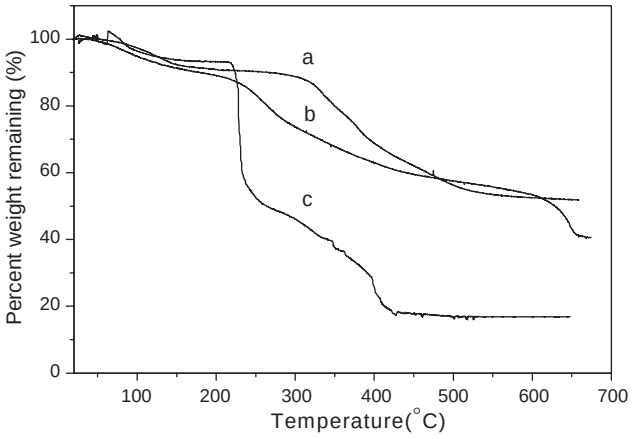

Fig. 6. TG curves for (a) Mg/Al-NO_3LDH, (b) SO_3-β-CD(6)/LDH and (c) $NaSO_3$-β-CD(6).

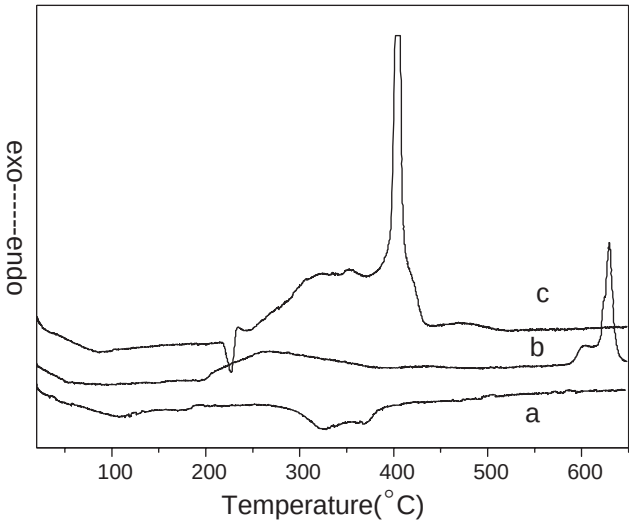

Fig. 7. DTA curves for (a) Mg/Al-NO_3LDH, (b) SO_3-β-CD(6)/LDH and (c) $NaSO_3$-β-CD(6).

the hydrogen bonding area as a result of deintercalation of interlayer water molecules. The second fall is from 200°C (1.384 nm) to 300°C (1.119 nm), which can be attributed to the decomposition of SO_3-β-CD(6) anions. The XRD patterns obtained in the range 350–500°C reveal that the LDH layer structure has broken down giving an amorphous material. The SO_3-β-CD(6) has decomposed completely at these temperatures which can be confirmed by the black color that the samples take on. From 600°C to 700°C the sample color becomes white indicating that combustion of the organic component has occurred. At temperatures above 400°C, reflections arising from a poorly crystalline MgO phase appear at about 43° and 63° (marked with +), as has been reported elsewhere [37].

The weak reflections around $2\theta = 14°$ and 28° appear to result from an impurity phase rather than a sublattice contribution, as their position does not alter as the temperature is raised from 20° to 400°C (Fig. 4).

The TG and DTA curves for the pure $NaSO_3$-β-CD(6), the Mg/Al-NO_3LDH precursor and the resulting SO_3-β-CD(6)/LDH complex are shown in Figs. 6 and 7 respectively. The $NaSO_3$-β-CD(6) precursor (Fig. 6c) exhibits three weight loss events. The first event (50–100°C) has been attributed to the loss of adsorbed and cavity water [19]; the second sharp event (200–230°C) is due to the decomposition of $NaSO_3$-β-CD(6) and is accompanied by an endothermic peak in the DTA curve (Fig. 7c); the third weight loss (230–420°C) is the result of combustion of $NaSO_3$-β-CD(6), with a corresponding strong exothermic peak in the DTA curve (Fig. 7c). The Mg/Al-NO_3LDH precursor also exhibits three weight loss stages. The first (100–120°C) and second (150–300°C) correspond to the removal of surface water (from both the internal gallery surface and the external surfaces); the third (300–520°C) is due to dehydroxylation of the brucite-like layers as well as decomposition of the NO_3^- anions [19]. The DTA curve is not very distinctive, showing two very weak endothermic peaks (Fig. 7a) at 320° and 370°C, respectively. The thermal decomposition of the SO_3-β-CD(6)/LDH complex is characterized by four steps (Fig. 6b): the first (90–150°C) is due to loss of both adsorbed water and SO_3-β-CD(6) cavity water molecules which is accordance with the variation in XRD patterns in this temperature range (Fig. 4); the second (150–250°C) is a consequence of both the decomposition of the SO_3-β-CD(6) anions which, by consideration of the changes in the d_{003} basal spacing of SO_3-β-CD(6), begins around 200°C (Fig. 5a) and the elimination of interlayer water, with a corresponding weak exothermic peak in the DTA curve (Fig. 7b); the third (250–540°C) can be attributed to dehydroxylation and decomposition of SO_3-β-CD(6) anions, which is complete at 300°C according to the

XRD patterns, and the collapse of the LDH structure above 350°C. The fourth stage (620–670°C) can be attributed to the combustion of SO_3-β-CD (6), with a corresponding strong exothermic peak in the DTA (Fig. 7b). Compared to the third stage decomposition of pure $NaSO_3$-β-CD(6) (Fig. 7c), the combustion temperature of interlayer SO_3-β-CD(6) is increased by some 250°C through intercalation. This significant increase in thermal stability of $NaSO_3$-β-CD(6) may be a result of the host–guest interactions present after intercalation or, since the IR spectra (vide supra) show little change on intercalation, may indicate that diffusion of oxygen is restricted by the presence of the host layers.

4. Conclusion

SO_3-β-CD(6)/LDH has been obtained by the intercalation of hexasulfated β-cyclodextrin into magnesium–aluminum layered double hydroxide by the method of ion exchange. XRD was used to confirm the intercalated structure, with $d_{003} = 1.578$ nm. Considering the dimensions of the β-cyclodextrin molecule and the rule of charge balance, the SO_3-β-CD(6) anions must adopt a monolayered arrangement with their cavity axis perpendicular to the LDH layer and sulfate groups on adjacent cyclodextrin molecules attached alternately to the upper and lower LDH layer surfaces. A schematic model of the intercalation structure has been proposed. The interaction between host and guest was investigated by FT-IR spectroscopy. The thermal decomposition of intercalated SO_3-β-CD(6) was investigated by variable temperature XRD and TG-DTA measurements. Compared with the pure form, the thermal stability of SO_3-β-CD(6) is enhanced after intercalation and its combustion temperature increased by 250°C.

Acknowledgments

This project was supported by the National Nature Science Foundation of China (No. 90206004).

References

[1] M. Meyn, K. Beneke, G. Lagaly, Inorg. Chem. 29 (1990) 5201.
[2] V.R.L. Constantino, T.J. Pinnavaia, Catal. Lett. 23 (1994) 361.
[3] A. Corma, V. Fornes, F. Rey, A. Cervilla, E. Llopis, A. Ribera, J. Catal. 152 (1995) 237.
[4] M. Ogawa, K. Kuroda, Chem. Rev. 95 (1995) 399.
[5] H. Tagaya, S. Sato, T. Kuwahara, J. Kadokawa, K. Masa, K. Chiba, J. Mater. Chem. 4 (1994) 1907.
[6] B. Sels, D. De Vos, M. Buntinx, F. Pierard, A. Kirsch-De Mesmaeker, P. Jacobs, Nature 400 (1999) 855.
[7] L. Ukrainczyk, M. Chibwe, T.J. Pinnavaia, S.A. Boyd, Environ. Sci. Technol. 29 (1995) 439.
[8] A.M. Fogg, V.M. Green, H.G. Harvey, D. O'Hare, Adv. Mater. 11 (1999) 1466.
[9] A.M. Fogg, J.S. Dunn, S.G. Shyu, D.R. Cary, D. O'Hare, Chem. Mater. 10 (1998) 351.
[10] M.L. Bender, M. Komiyama, Cyclodextrin Chemistry, Springer, Berlin, 1978.
[11] X. Wang, M.L. Brusseau, Environ. Sci. Technol. 29 (1995) 2632.
[12] E. Fenyvesi, J. Szeman, J. Szejtli, J. Incl. Phenom. 25 (1996) 229.
[13] Y. Inoue, T. Hakushi, Y. Liu, L.H. Tong, B.J. Shen, D.S. Jin, J. Am. Chem. Soc. 115 (1993) 475.
[14] J. Szejtli, J. Incl. Phenom. Mol. Recognit. Chem. 14 (1992) 25.
[15] I. Tabushi, Tetrahedron 40 (1984) 269.
[16] E.V. Akkaya, A.W. Czarnik, J. Am. Chem. Soc. 110 (1988) 8553.
[17] T. Kijima, J. Tanaka, Y. Matsui, Nature 310 (1984) 45–47.
[18] T. Kijima, Y. Matsui, Nature 322 (1986) 533–534.
[19] H.T. Zhao, G.F. Vance, J. Chem. Soc., Dalton Trans. 11 (1997) 1961–1965.
[20] H.T. Zhao, G.F. Vance, Clays Clay Miner. 46 (1998) 712–718.
[21] S. Mayer, M. Schleimer, V. Schurig, J. Microcol. Sep. 6 (1994) 43–48.
[22] R.J. Tait, D.O. Thompson, V.J. Stella, J.F. Stobaugh, Anal. Chem. 66 (1994) 4013–4018.
[23] F.A. Chen, R.A. Evangelista, J. Chin. Chem. Soc. 46 (1999) 847.
[24] C. Perrin, Y.V. Heyden, M. Maftouh, D.L. Massart, Electrophoresis 22 (2001) 3203–3215.
[25] V.R.L. Constantino, T.J. Pinnavaia, Inorg. Chem. 34 (1995) 883.
[26] Z. Ruan, J. You, Chin. J. Chromatogr. 18 (2000) 184–186.
[27] F. Cavani, F. Trifiro, A. Vaccari, Catal. Today 11 (1991) 173.
[28] S. Miyata, Clays Clay Miner. 23 (1975) 369.
[29] J. Szejtli, Cyclodextrins and their Inclusion Complexes, Akademiai Kiado, Budapest, 1982.
[30] N.T. Whilton, P.J. Vickers, S. Mann, J. Mater. Chem. 7 (1997) 1623–1629.
[31] A. Fudala, I. Palinko, I. Kiricsi, Inorg. Chem. 38 (1999) 4653–4658.
[32] C.O. Oriakhi, I.V. Farr, M.M. Lerner, J. Mater. Chem. 6 (1996) 103.
[33] I. Bratu, S. Astilean, C. Ionesc, E. Indrea, J.P. Huvenne, P. Legrand, Spectrochim. Acta Part A 54 (1998) 191–196.
[34] G. Zundel, Hydration and Intermolecular Interaction, Academic Press, New York, 1969.
[35] J. Pérez-Ramírez, G. Mul, F. Kapteijn, J.A. Moulijn, J. Mater. Chem. 11 (2001) 821.
[36] H.D. Ruan, R.L. Frost, J.T. Kloprogge, L. Duong, Spectrochim. Acta Part A 58 (2002) 265–272.
[37] E. Kanezaki, Solid State Ionics 106 (1998) 279.